XII International Conference on Computational Plasticity. Fundamentals and Applications
COMPLAS XII
E. Oñate, D.R.J. Owen, D. Peric and B. Suárez (Eds)

MULTISCALE MATERIAL MODEL FOR ASR-AFFECTED CONCRETE STRUCTURES

R. ESPOSITO* AND M.A.N. HENDRIKS*†

*Department of Structural Engineering
Delft University of Technology
Stevinweg 1, 2628 CN, Delft, The Netherlands
e-mail: r.esposito@tudelft.nl, m.a.n.hendriks@tudelft.nl
web page: http://www.citg.tudelft.nl

†Norwegian University of Science and Technology (NTNU)
Rich. Birkelandsvei 1A, 7491 Trondheim, Norway
e-mail: max.hendriks@ntnu.no - Web page: http://www.ntnu.no

Key words: Alkali-Silica Reaction (ASR), Multiscale model, Micromechanics, Damage

Abstract. One of the most harmful degradation process for concrete structures is the alkali-silica reaction. This process starts at aggregate level with a gel swelling and can produce damage up to macro level, by compromising the integrity and capacity of the structure. In order to better understand the complex nature of this phenomenon, a multiscale material modeling approach is presented. The aim of the model is to capture the coupled effect between chemical and mechanical loading on stiffness, strength and expansion. To this end the chemical loading is driven by a gel production, within a micromechanical damage model. After summarizing the main features on the model, a numerical example illustrates the use of the model for uniaxial tensile tests.

1 INTRODUCTION

The sustainability and serviceability of concrete structures has become highly relevant. Adequate modeling is important when engineers have to deal with long term deterioration processes. One of these phenomena is the Alkali-Silica Reaction (ASR), that is the chemical process between the alkali available in the cement and the silica in the aggregates.

Its product is a hydrophilic gel which swells and causes damage, possibly influencing the integrity and capacity of the structure. The expansion process is strongly linked to the stress state of the structure [1, 2] and it indeed results in the degradation of the mechanical properties [3].

The micromechanical nature of ASR has a complex effect on the macromechanical behavior of the concrete. For a proper understanding and implementation of ASR a

multiscale approach is presented. In this the driving parameter of the chemical loading is the gel production. This allows to describe the ASR effects on the mechanical properties and its relation with the mechanical loading conditions.

It has been observed that the swelling process of a sample in free expansion condition is influenced by the type of aggregate and cement employed, the environmental conditions, the distribution of the microcracks [4] and the aggregate size [5]. Models which use the macroscopic expansion strain as a driving parameter for the chemical loading consider all these parameters as intrinsic material properties and are usually amounted to the specification of an expansion curve [4]. In this way the behavior of a structure, in which chemical and mechanical loading are coupled, is modeled by explicitly introducing additional relationships to describe stress-induced anisotropic effects and the degradation of mechanical properties (viz. stiffness and strength) [2, 1]. By considering, in contrast, the gel production as driving parameter, stress-induced anisotropy and mechanical degradation are outcomes of the multiscale model and can be determined for any loading condition.

The micromechanical approach is based on an idea proposed by Lemarchand et al. [6] and further developed by Charpin and Ehrlacher [7]. The concrete is modeled, at micro level, as a heterogeneous material: aggregates and cracks filled by the gel are considered as embedded inclusions in the cement paste, that is the matrix. It is assumed that the gel formation starts at the rim between aggregates and cement paste and that subsequently the gel flows through the matrix pressurizing and damaging the cracks. The aggregate and the surrounding gel are modeled by spherical inclusions; the cracks as ellipsoidal inclusions. The effective stiffness properties of the medium are evaluated by the Mori-Tanaka homogenization scheme [8]. The expansion of the concrete as a result of the gel swelling is modeled with the poromechanics theory [9] The micromechanical damage propagation is based on linear fracture mechanics theory [9].

In this paper the coupling phenomenon between the internal ASR loading and the external mechanical loading is presented by considering subsequential ASR loading and mechanical loading. Before that, section 2 presents the micromechanical model with gel-pressurizing inclusions, and section 3 links the gel pressure with the gel production.

2 MICROMECHANICAL MODEL OF CONCRETE

The multiscale material model evaluates the properties of ASR-affected concrete on the basis of a micromechanical aspects and analyses the behavior of a Representative Elementary Volume (REV).

The concrete is modeled as an heterogeneous material composed by aggregates and microcracks embedded in the cement paste. The bond between the aggregate and the cement paste is described by an interfacial transition zone (ITZ), which has a thickness, l_{ITZ}, between 50 and 100 micron. The aggregates and their surrounding ITZ are modeled as spheres, named inclusions type 1 (Figure 1). The model allows to consider m_1 families of inclusion type 1, which differ in radius r_i ($= R_a^i + l_{ITZ}$) and volume fraction ϕ_{1i}. In the example a single family ($m_1 = 1$) will be assumed. The microcracks are modeled by m_2

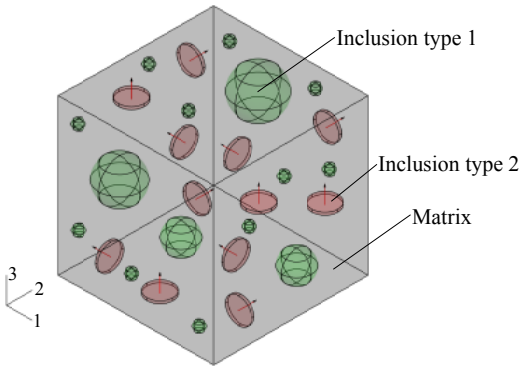

Figure 1: Three phase material model.

families of penny-shaped inclusions (inclusions type 2), with radius a_i in the inclusion's plane and radius c_i in thickness direction. The shape of these inclusions can be described also by the aspect ratio:

$$X_i = \frac{c_i}{a_i} \tag{1}$$

Their volume fraction is:

$$\phi_{2i} = \frac{4}{3}\pi n_i a_i^3 X_i \tag{2}$$

where n_i is the number of crack per unit of volume of the i-th family of inclusion type 2.

The alignment of the microcracks is relevant for the estimation of the overall stiffness. Rather than a single family with a random orientation, three families of inclusions type 2 ($m_2 = 3$) are considered. Within each family the cracks are aligned in one plane with normal $\boldsymbol{n}_i$. Three orthogonal crack planes are considered. In an undamaged concrete, the initial thin microcracks have similar aspect ratio X_i and volume fraction ϕ_{2i} for the three planes. In a later stage we might reconsider this to model intrinsic orthotropy, which can lead to an anisotropic swelling of ASR-affected concrete in free expansion conditions [4].

2.1 Development of alkali-silica reaction gel

The ASR is the chemical process between the alkali available in the cement and the silica in the aggregates, which produces an hydrophilic gel which swells and causes damage, possibly influencing the integrity and capacity of the structure. It is assumed that the reaction starts at the rim between aggregates and cement paste. In the first stage of the reaction the gel (Figure 2b), which has a volume δ times bigger then the volume of the reagents which created it, occupies the space left free from the erosion of the aggregates and the interfacial zone. The latter is the most porous zone in the concrete, and can therefore be easily occupied by the gel.

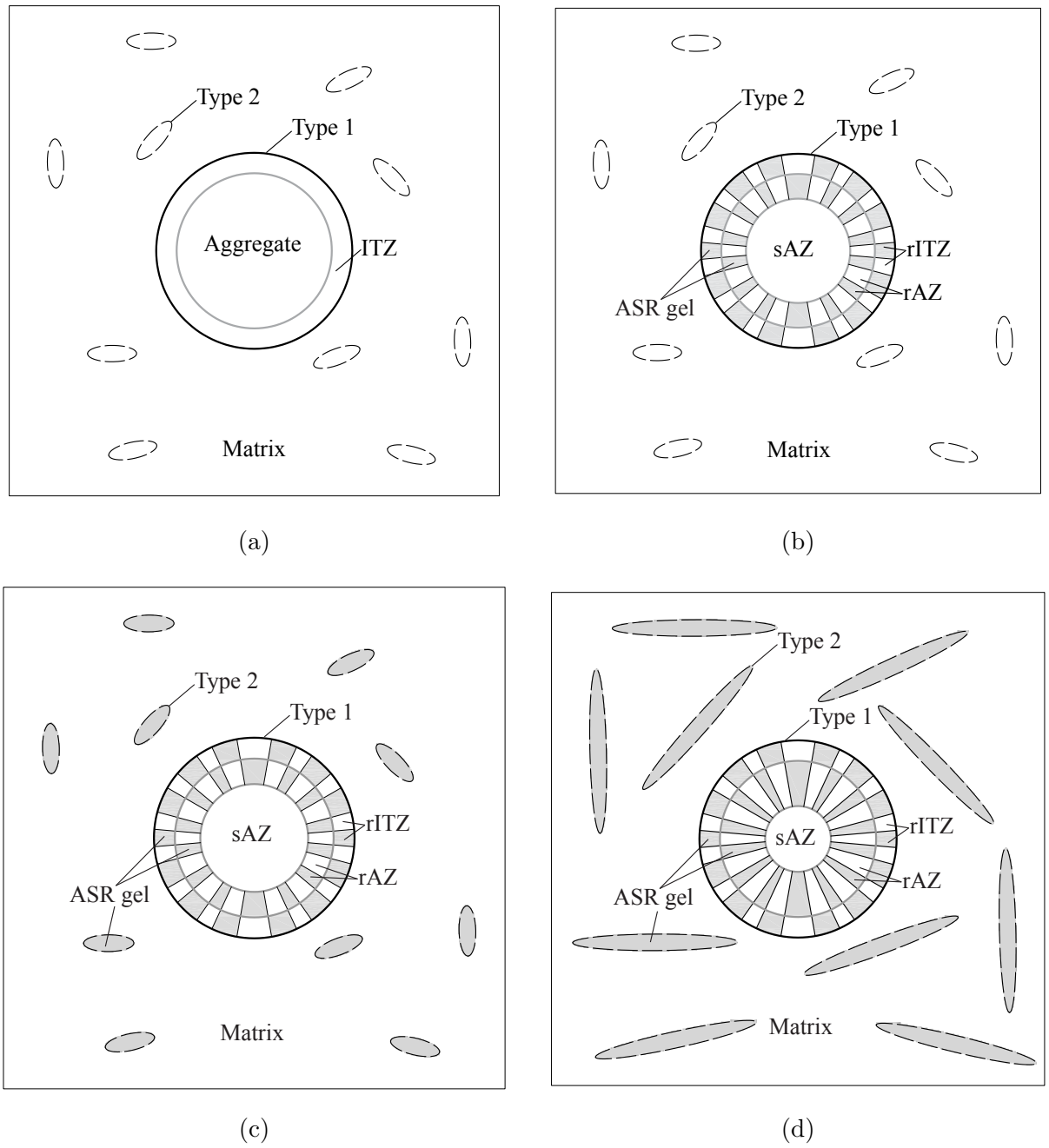

Figure 2: Microstructural evolution in ASR-affected concrete (2D visualization for a randomly oriented type 2 family). (a) Unaffected concrete; (b) First stage: Beginning of the reaction; (c) Second stage: Filling of the cracks; (d) Third stage: Propagation of the cracks.

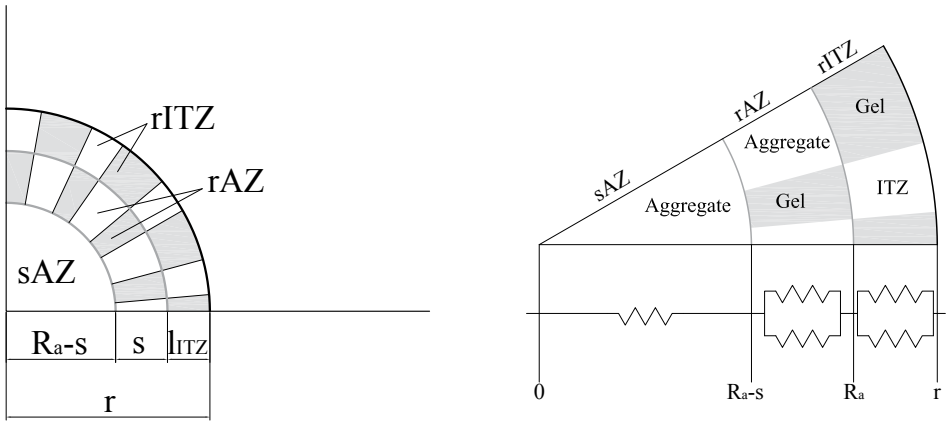

Figure 3: Inclusion type 1 (2D visualization): (a) Composition; (b) Mechanical behavior.

The inclusion type 1 changes composition while the reaction evolves; it is possible to identify three zones (Figure 3a):

- a sound aggregate zone (sAZ) composed by aggregate material only;
- a reactive aggregate zone (rAZ) composed by aggregate and gel material;
- a reactive interfacial transition zone (rITZ) composed by ITZ and gel material.

It is assumed that the materials in the three zones work as springs placed in series and that in each zone the materials work as spring placed in parallel (Figure 3b).

When the zone surrounding the aggregate is saturated and the pressure P produced by the gel is higher than the micromechanical tensile strength of the cement paste f_{0t}, the gel flows into the microcracks (Figure 2c) and only when they are complete filled the gel starts damaging the matrix. The cracks are modeled by penny shaped inclusions fully saturated and embedded in the matrix. It is assumed that the cracks develop in the cement paste by increasing their crack radius, a (Figure 2d).

In order to describe the amount of gel produced in time, the attacked depth s of each family of inclusion type 1 is defined as [7]:

$$s\left(t\right) = \alpha^{i}\left(t, R_{a}^{i}\right) R_{a}^{i} \tag{3}$$

where R_a^i and α^i are, respectively, the aggregate radius and the reaction ratio of the i-th family of inclusion type 1. Time evolution laws for the reaction ratio have been proposed by several researchers (e.g. Multon et al.[5] and Charpin and Ehrlacher [7]). In this paper the capability of the model are investigated by considering different reaction ratios α; at the moment the time dependency is not taken into account.

2.2 State equations and damage criterion

At any stage the concrete can be subjected both to an external mechanical load and to the internal chemical load, that is the pressure P developed by the ASR gel. The behavior of a REV subjected to a mechanical load defined by uniform strain boundary conditions (macroscopic strain $\boldsymbol{E}$) and to a fluid pressure P can be described by Biot theory [9]. The state equations which characterize the linear poroelastic behavior read:

$$\begin{aligned} \boldsymbol{\Sigma} &= \mathbb{C} : \boldsymbol{E} - \boldsymbol{B}P \\ \Phi - \Phi_{in} &= \frac{P}{N} + -\boldsymbol{B} : \boldsymbol{E} \end{aligned} \tag{4}$$

where $\boldsymbol{\Sigma}$ is the macroscopic stress and $(\Phi - \Phi_{in})$ is the variation of the volume in which the pressure is developed. The overall drained stiffness tensor $\mathbb{C}$ is defined through Mori-Tanaka homogenization scheme [8]. It depends from the elastic properties of the matrix and each inclusion family and from the volume fractions and shapes of the inclusions. The Biot coefficient $\boldsymbol{B}$ and modulus N are defined as:

$$\begin{aligned} \boldsymbol{B} &= \boldsymbol{I} : \left(\mathbb{I} - \mathbb{C}_0^{-1} : \mathbb{C}\right) \\ \frac{1}{N} &= (\boldsymbol{B} - \Phi \boldsymbol{I}) : \mathbb{C}_0^{-1} : \boldsymbol{I} \end{aligned} \tag{5}$$

with $\mathbb{C}_0$ the stiffness tensor of the matrix phase and $\boldsymbol{I}$ and $\mathbb{I}$ the 2nd and 4th order unit tensor, respectively.

The crack propagation is described by the damage criterion, which is formulated in the framework of linear fracture mechanics theory, on the basis of thermodynamic concepts [9]. The macroscopic dissipation is a function of the potential energy Ψ of the system, which reads:

$$\Psi\left(\boldsymbol{E}, P, \epsilon\right) = \frac{1}{2}\boldsymbol{E} : \mathbb{C} : \boldsymbol{E} - \frac{P^2}{2N\left(\epsilon\right)} - P\boldsymbol{B}\left(\epsilon\right) : \boldsymbol{E} \tag{6}$$

where ϵ is the damage parameter related to each family of inclusions type 2. Skipping the family index for convenience, this damage parameter can be expressed as [10]:

$$\epsilon = na^3 \tag{7}$$

The driving force of the damage process is the energy release rate G:

$$G\left(\boldsymbol{E}, P, \epsilon\right) = \frac{\partial \Psi}{\partial \epsilon} = -\frac{1}{2}\boldsymbol{E} : \frac{\partial \mathbb{C}\left(\epsilon\right)}{\partial \epsilon} : \boldsymbol{E} - \frac{P^2}{2}\frac{\partial}{\partial \epsilon}\left(\frac{1}{N\left(\epsilon\right)}\right) - P\frac{\partial \boldsymbol{B}\left(\epsilon\right)}{\partial \epsilon} : \boldsymbol{E} \tag{8}$$

By introducing Eqs. 6 in 8, the energy release rate reads:

$$G\left(\boldsymbol{E}, P, \epsilon\right) = -\frac{1}{2}\left(\boldsymbol{E} + P\mathbb{C}_0^{-1} : \boldsymbol{I}\right)\frac{\partial \mathbb{C}\left(\epsilon\right)}{\partial \epsilon}\left(\boldsymbol{E} + P\mathbb{C}_0^{-1} : \boldsymbol{I}\right) \tag{9}$$

where $\boldsymbol{E}' = \left(\boldsymbol{E} + P\mathbb{C}_0^{-1} : \boldsymbol{I}\right)$ is the effective strain controlling the damage. Making use of Eqs. 5 and 6, the effective stress results in:

$$\boldsymbol{\Sigma}' = \mathbb{C} : \left(\boldsymbol{E} + P\mathbb{C}_0^{-1} : \boldsymbol{I}\right) = \boldsymbol{\Sigma} + P\boldsymbol{I} \tag{10}$$

The driving force as a function of the effective stress then becomes:

$$G\left(\boldsymbol{\Sigma}, P, \epsilon\right) = -\frac{1}{2}(\boldsymbol{\Sigma} + P\boldsymbol{I}) : \mathbb{D}\left(\epsilon\right) : \frac{\partial \mathbb{C}\left(\epsilon\right)}{\partial \epsilon} : \mathbb{D}\left(\epsilon\right) : (\boldsymbol{\Sigma} + P\boldsymbol{I}) \tag{11}$$

with $\mathbb{D}$ the overall drained compliance tensor.

Crack propagation will occur only if the driving force results higher than the critical energy release rate G_c of the current system; thus the damage criterion reads:

$$\begin{aligned} G(\boldsymbol{E}, P, \epsilon) &\geq G_c(\epsilon) \\ G(\boldsymbol{\Sigma}, P, \epsilon) &\geq G_c(\epsilon) \end{aligned} \tag{12}$$

The critical energy release rate G_c can be expressed as function of the current damage parameter ϵ [9]:

$$G_c = \frac{2\pi}{3} G_f \left(\frac{n}{\epsilon}\right)^{1/3} = \frac{2\pi}{3}\frac{G_f}{a} \tag{13}$$

with G_f the fracture energy, which is a material parameter.
For a known macroscopic strain $\boldsymbol{E}$ (or stress $\boldsymbol{\Sigma}$) and a known damage parameter ϵ, Eq. 12 defines a limiting admissible pressure level, $P_{lim}\left(\epsilon\right)$.

In order to study the crack propagation in the REV, the damage criterion should be verified for each family of inclusions type 2, each one being associated with a damage parameter ϵ_i.

3 ESTIMATION OF THE GEL PRESSURE

The pressure is determined by considering the mass equilibrium. By assuming that the gel has a volume δ time bigger than the one of its reagents and that it is confined into the concrete skeleton, the gel pressure can be estimated by:

$$V_{gu}\left(1 - \frac{P}{K_{gel}}\right) = V_{avail} \tag{14}$$

where K_{gel} is the bulk modulus of the gel, V_{avail} is the available volume and V_{gu} is the unpressurized gel volume:

$$V_{gu} = \sum_{i=1}^{m_1} \delta N_{agg}^i \rho_1 V_{rAZ}^i \tag{15}$$

where m_1 are the families of inclusion type 1 in the REV. V^i_{rAZ} is the volume of the i-th reactive aggregate zone of which a volume fraction ρ_1 has been reacted. N^i_{agg} is the number of aggregate in the REV for the i-th family of inclusion 1.

The available volume depends from the reaction stage. In the first stage the gel, created at the rim, flows into the available space in inclusion type 1 (Figure 2b), occupying the volume left free by the erosion of the aggregates and the porosity volume of the interfacial transition zone:

$$V_{1a} = \sum_{i=1}^{m_1} N^i_{agg} \left(\rho_1 V^i_{rAZ} + \rho_2 V^i_{rITZ} \right) \tag{16}$$

where V^i_{rITZ} is the volume of the reactive interfacial zone of the i-th family of inclusion type 1, and ρ_2 is the corresponding volume fraction of the gel.

In the second stage, as the pressure P reaches the tensile strength of the cement paste f_{0t}, the gel flows into the inclusions type 2 (Figure 2c), which have a total volume equal to:

$$V_{2a} = V_{REV} \sum_{i=1}^{m_2} \frac{4}{3} \pi n_i a_i^3 X_i \tag{17}$$

where m_2 are the families of inclusion type 2 in the REV characterized by a crack radius a_i, an aspect ratio X_i (Eq. 1) and amount per unit of volume n_i.

In the third stage (Figure 2d) the damage occurs and the crack radius a of all families of inclusions type 2 is incremented by imposing that the pressure is equal to the threshold pressure P_{lim} evaluated, for the current value of reaction ratio α and damage parameter ϵ, through the damage criterion (Eq. 12).

From Eqs. 14-17 the gel pressure reads:

$$P(\alpha) = \begin{cases} \left(1 - \frac{V_{1a}}{V_{gu}}\right) K_{gel} & \text{first stage} \\ \left(1 - \frac{V_{1a}+V_{2a}}{V_{gu}}\right) K_{gel} & \text{second and third stages} \end{cases} \tag{18}$$

Note that Eq. 18 is an implicit equation in the damage parameter ϵ. The pressure P, at the left hand side, should obey Eq. 12 such that $P \leq P_{lim}(\epsilon)$. The available volume V_{2a} on the right hand side depends on the damage parameter ϵ since the crack radius a_i depends on it.

4 NUMERICAL EXAMPLE

In this section the model is applied to a ASR-affected concrete sample in free expansion condition. The attention is focused on the estimation of the expansion and the degradation of mechanical properties as a function of the reaction ratio α. In this example only one

family of inclusions 1 is defined ($m_1 = 1$). Three families of inclusions type 2 ($m_2 = 3$), with the same crack radius a ($= a_1 = a_2 = a_3$) and equally distributed in the three orthogonal crack planes ($n_1 = n_2 = n_3 = n$) are considered.

At the initial step the microstructure of the unaffected concrete (in terms of aspect ratio and volume fraction of inclusion type 2) is determined by fitting the initial value of the Young's modulus of concrete E_{in} (which is an input data of the model). The fracture energy G_f is determined through the damage criterion (Eq. 12) by imposing that the stress which will cause crack propagation, in an uniaxial tensile test, is equal to the tensile strength $f_{t,in}$ of the unaffected concrete.

At each step the gel pressure, P is estimated through Eq. 18. If the damage criterion (Eq. 12) is satisfied, the threshold pressure P_{lim} and the crack radius a are updated. It is assumed that for ASR-affected concrete in free expansion condition, the crack placed along three directions are growing simultaneously and in the same manner. Figure 4a and 4b show the variation of the pressure P and of the crack radius a as a function of the reaction ratio, α.

The mechanical properties are estimated by performing an uniaxial tensile test along $\boldsymbol{n}_3$ axis. In this way it is possible to estimate for each value of the reaction ratio α, the expansion, the tensile strength and the stiffness. Figure 4c shows the results of the uniaxial tensile test in terms of effective stress $\boldsymbol{\Sigma'}$ and strain $\boldsymbol{E'}$ for different reaction ratios, α. Note that the the model is able to predict the post-peak behavior of sound concrete subjected to mechanical loading ($\alpha = 0$). A clear degradation of both strength and stiffness is observed for increasing values of α.

The overall behavior is summarized in Figure 4d in terms of ratio with respect to the initial value (for the tensile strength and stiffness) or the maximum value (for the expansion strain). The model is able to capture the different degradation rate for stiffness and strength, as reported in literature [3].

5 CONCLUSION

The alkali-silica reaction in concrete is a harmful deterioration, which starts at aggregate level and can compromise the durability and serviceability of the structure. The micromechanical nature of ASR has a complex effect in the macromechanical behavior of the concrete. For a proper understanding and implementation of ASR a multiscale material model is presented. This approach uses the gel production as driving parameter of ASR. This allows to model the interaction between chemical and mechanical loading on the mechanical properties. As already proposed by Lemarchand et al. [6] and by Charpin and Ehrlancher [7], a micromechanical model of concrete is introduced to explain the development of ASR gel. The concrete, at micro level, is modeled as an heterogeneous material composed by aggregate and microcracks embedded in the cement paste. The crack propagation is simulated by increasing of the crack radius, a. The damage process is controlled by the damage criterion expressed in terms of effective stress or effective strain.

Table 1: Input and initial parameters of the model.

Input parameters		
Initial young's modulus of concrete, E_{in}	38600	MPa
Initial tensile strength of concrete, $f_{t,in}$	2.35	MPa
Initial tensile strength of cement paste, f_{0t}	4.0	MPa
Young's modulus of aggregates, E_{agg}	70000	MPa
Young's modulus of ITZ, E_{ITZ}	15000	MPa
Young's modulus of cement paste, E_{cp}	25000	MPa
Bulk modulus of the gel, K_{gel}	2150	MPa
Poisson ratio, ν	0.2	
Aggregate radius, R_a	5.0	mm
ITZ thickness, l_{ITZ}	0.1	mm
Volume fraction of aggregate, F_{agg}	0.6	
Crack thickness, $c = c_1 = c_2 = c_3$	$0.50\ 10^{-3}$	mm
Volume swelling ratio, δ	1.1	
Gel volume fraction		
in rAZ, ρ_1	0.2	
in rITZ , ρ_2	0.2	
Calibrated initial parameters		
Number of cracks per unit of volume		
total, $n_{tot} = 3n$	$6.72\ 10^{-2}$	
for each family, $n = n_1 = n_2 = n_3$	$2.24\ 10^{-2}$	
Initial volume fractions		
type 1, ϕ_1	$6.37\ 10^{-1}$	
type 2, $\phi_2 = \phi_{2,1} + \phi_{2,2} + \phi_{2,3}$	$3.15\ 10^{-5}$	
Initial aspect ratio, $X = X_1 = X_2 = X_3$	$6.10\ 10^{-4}$	
Initial crack radius, $a = a_1 = a_2 = a_3$	$8.20\ 10^{-1}$	mm
Initial damage parameter, $\epsilon = \epsilon_1 = \epsilon_2 = \epsilon_3$	$1.23\ 10^{-2}$	
Fracture energy, G_f	$1.34\ 10^{-4}$	N/mm
Initial threshold pressure, $P_{lim}(\alpha = 0)$	1.35	MPa

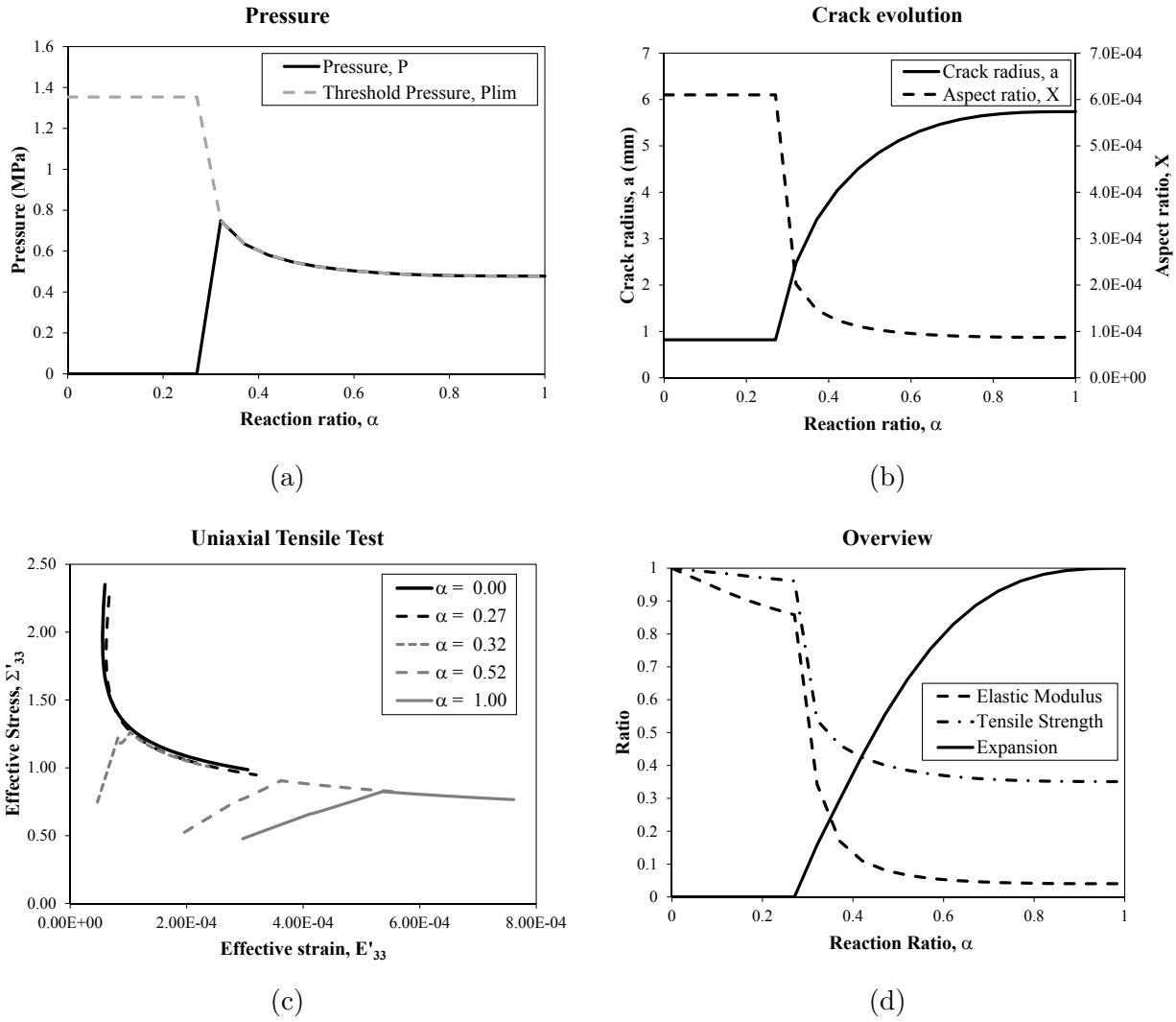

Figure 4: Numerical results: Pressure (a) and damage (b) developed during ASR-swelling in free expansion; uniaxial tensile tests for five different reaction ratios (c); normalized results for stiffness, strength and expansion (d).

It turns out that the model is able to describe the behavior of ASR-affected concrete samples in free expansion condition, in terms of both expansion and degradation of mechanical properties. The different degradation rate between stiffness and strength, reported by several researchers, is also an outcome of the model. This feature of the model can be employed in a structural analysis which has as driving parameter the gel production. The model allows studying the coupling phenomenon between the internal ASR loading and the external mechanical loading.

REFERENCES

[1] Multon, S. and Toutlemonde, F. Effect of applied stresses on alkali-silica reaction-induced expansions. *Cement and Concrete Research* (2006) **36**(5):912-920.

[2] Saouma, V. and Perotti, L. Constitutive model for alkali-aggregate reactions. *ACI Materials Journal* (2006) **103**(3):194-202.

[3] Esposito, R. and Hendriks, M.A.N. A Review of ASR modeling approaches for Finite Element Analyses of dam and bridges. In *14th International Conference on Alkali Aggregate Reaction*, Austin, Texas (2012).

[4] Larive, C. *Apports combinas de l experimentation et de la modellisation la comprehension de l'alcali-reaction et de ses effets mecaniques*. LCPC (1998).

[5] Multon, S., Cyr, M., Sellier, A. and Diederich, P. and Petit, L. Effects of aggregate size and alkali content on ASR expansion. *Cement and Concrete Research* (2010) **40**(4):508-516.

[6] Lemarchand, E., Dormieux, L., Ribeiro, F. and Fairbairn, E. A micromechanical approach to ASR-induced damage in concrete. In *Poromechanics III - Biot Centennial (1905-2005)*, Taylor & Francis (2005).

[7] Charpin, L. and Ehrlacher, A. A computational linear elastic fracture mechanics-based model for alkali-silica reaction. *Cement and Concrete Research* (2012) **42**(4):613-625.

[8] Mori, T. and Tanaka, K. Average stress in matrix and average elastic energy of materials with misfitting inclusions. *Acta Metallurgica Et Materialia* (1973) **21**:571-574.

[9] Dormieux, L. and Kondo, D. Poroelasticity and damage theory for saturated cracked media. In *Applied micromechanics of porous materials*. SpringerWienNewYork, (2005).

[10] Budiansky, B. and O'connell, R.J. Elastic moduli of a cracked solid. *International Journal of Solids and Structures* (1976) **12**(2):81-97.